Adv. Geosci., 65, 83–101, 2024
https://doi.org/10.5194/adgeo-65-83-2024

Advances in Geosciences
Open Access
EGU

Storm Daria: Societal and energy impacts in northwest Europe on 25–26 January 1990

Anthony J. Kettle

Météo-France, Centre de Météorologie Spatiale, Avenue de Lorraine, 22300 Lannion, France

Correspondence: Anthony J. Kettle (ake3358@gmail.com)

Received: 27 June 2024 – Revised: 17 October 2024 – Accepted: 17 October 2024 – Published: 13 December 2024

Abstract. Between late January and early March of 1990 Europe was hit by a sequence of severe winter storms that caused significant infrastructure damage and a large number fatalities. The storm sequence started with Hurricane Daria on 25–26 January 1990, which was one of the most serious events of the storm cluster, especially for the UK. The low pressure centre moved in a west-northwest direction across Ireland, southern Scotland, and north of Denmark before moving further into the Baltic. The strongest winds south of the trajectory path caused significant damage and disruptions in England, France, Belgium, the Netherlands, and West Germany. Media reports highlighted building damage, interrupted transportation networks, power outages, and fatalities. There were also a series of maritime emergencies in the Bay of Biscay, English Channel, North Sea, and Baltic Sea. This contribution takes a closer look at Storm Daria, presenting an overview of meteorological measurements and the societal impacts, followed by an analysis of the North Sea tide gauge network to understand the storm surge and possible large wave occurrences. Offshore wind energy was at the planning stage in this early period, but onshore wind energy was established in Denmark with demonstration projects in other countries. The storm is an important case study of extreme meteorological conditions that can impact energy infrastructure.

1 Introduction

In the list of severe European winter wind storms of recent decades, Storm Daria (also called the Burn's Day Storm) from January 1990 and Storm Lothar from December 1999 appear near the top for the damage costs and the number of fatalities (Swiss Re, 2018). Storm Daria appears in the first rank for damage costs, but Storm Lothar is a close second, and Lothar had a higher number of fatalities. Both storms took place during an early stage of wind energy development in Europe, and the impacts on wind energy infrastructure were not large. However, it is important to revisit storms like these to understand their potential impact on wind energy and offshore wind energy in particular. In spite of the damage caused by Storm Lothar, it would not be considered a major storm for European offshore wind energy because its trajectory passed eastward across northern France and Germany, so that its most destructive wind field occurred south of the North Sea coast where most offshore wind infrastructure is presently located. In contrast, the trajectory of Storm Daria passed across Scotland and the central North Sea, and its destructive wind field included coastal regions in the southern North Sea between the UK and Denmark. This storm had significant offshore and coastal impacts in Europe, and is relevant for understanding the risks for offshore wind energy.

The year 1990 was an important turning point in the public awareness of the climate change problem. It was the year of publication of the first report of the Intergovernmental Panel on Climate Change (IPCC) by Houghton et al. (1990). The IPCC had been convened in 1988 to assess the case of anthropogenic climate warming through the emission of greenhouse gases, primarily by fossil fuel combustion. In the early 1980s, global average surface temperatures, which had shown fluctuations on different time scales over the preceding century, exceeded the previous record from the mid-1940s. There was some indication that climate warming from atmospheric greenhouse gases had emerged from the background of cyclical climate variability. James Hansen, a senior climate modeller in the NOAA government department of the USA, made high profile statements to government panels about the scientific evidence supporting climate change

(Supran et al., 2023). Although the climate change predictions from the IPCC and scientific community initially faced opposition from the fossil fuel industry (Hansen, 2009), there was increased government support for alternative energy programs in Europe following the first IPCC report in 1990. The rapid growth of onshore wind energy dates from the early 1990s. Before 1990, a number of countries had small-scale experimental wind energy programs, but only Denmark and the US state of California had carried this forward with the construction of thousands of wind turbines from the early 1980s to supply a significant fraction of their electricity requirements (Auken, 2002). Feasibility studies for offshore wind farms in Europe started in the early 1980s (International Energy Agency, 1981), but the first experimental offshore turbines were only erected in coastal areas in the early 1990s, and Horns Rev in Denmark became the first large scale operational offshore wind farm in 2002 (Beurskens, 2014).

Storms were anticipated to increase as the effects of climate change became apparent (Hansen, 2009). This was flagged at an early stage by several economic sectors. The insurance industry placed special emphasis on the occurrence of severe weather events that crossed the threshold of 1 billion dollars (USD) of insured losses (Berz, 1998). This started in 1984 with Hurricane Alicia in the US, and accelerated in the 1990s with a number of severe storms in Europe and the US. The trend of increasing damage costs had several contributing factors, including population increases, the construction of building assets in susceptible areas, as well as the occurrence of storms of increasing severity (Berz, 1998, 1999, 2005). In Europe, a series of winter storms during the first months of 1990 were important in defining the insurance loss trend in the early period. At the time it occurred in January 1990, winter storm Daria topped the world list of USD 1 billion insurance loss storms. However, severe cyclones were also occurring in other parts of the world, and Storm Daria was displaced from its rank 1 position first by Japanese Typhoon Mireille in 1991 and then by Hurricane Andrew in 1992.

The issue of maritime storms and sea state had also been flagged by offshore industries at an earlier date. In the aftermath of the 1982 loss of the drilling rig *Ocean Ranger* in a winter storm off Newfoundland, Neu (1984) made an analysis of wave charts from 1970 to 1982 and found increases in significant wave heights across the period. The results were broadly supported by Bouws et al. (1996) using a larger number of wave charts from the Netherlands meteorological office KNMI over the period 1960 to 1988, and they suggested a link with the North Atlantic Oscillation. Reviewing the sea state literature based on the observational network from the North Atlantic and North Sea, Bacon and Carter (1991) indicated that the trend toward increasing storminess in the North Atlantic could be traced back to the early 1950s. However, WASA group (1998) highlighted that the issue of data inhomogeneities might have introduced spurious trends in the earlier studies, and suggested that long time series of atmospheric pressure from fixed meteorological stations provided a better metric to understand storminess patterns. Using this data source, decadal trends of variability were highlighted, and the heightened storminess of the 1980s and 1990s was comparable to sea states from the late 19th century.

Linked with the worsening sea state, rogue wave strikes on shipping and offshore infrastructure were also highlighted in the 1990s. This led to the high profile research program MAXWAVE (Rosenthal, 2005) in the period 2000–2003 as well as themed conferences in 2000, 2004, and 2008 targeting rogue wave issues (Olagnon and Athanassoulis, 2001; Olagnon and Prevosto, 2005, 2009). Rogue waves had always been known, but before the first continuous instrument records in the 1960s (Draper, 1964), it was difficult to characterize their frequency or dynamics. A series of rogue wave papers appeared in the 1970s, mainly linked with shipping issues (Mallory, 1974; Atkins, 1977). In the North Sea, the Norwegian petroleum safety authority catalogued wave strikes on the 20 m working deck of production platforms during bad storms starting from the early 1980s (Hamre et al., 1991), with a particularly damaging storm taking place in December 1990 (Kvitrud, 1997). The list is notable because the platform deck heights were designed for extreme wave strikes that should only have been taking place statistically on century time scales. When the MAXWAVE program started in 2000, shipping accidents caused by rogue waves were appearing regularly in the media for their damage to passenger ships, and the loss of the ferry *Estonia* during a Baltic Sea storm in September 1994 was the worst example (Faulkner, 2002). In spite of the record of shipping damage, research into the frequency and general size characteristics of rogue waves has progressed slowly. As outlined by Liu and MacHutchon (2006), the problem is the availability of raw and uncontrolled high frequency recordings of waves. Most rogue wave research is based on a very small number of case studies that have been released to the scientific community, and the *Draupner* wave during a North Sea storm on 1 January 1995 (Haver, 2005) is the best known. Large amounts high frequency wave data have been recorded on offshore platforms, but it is generally not available to the scientific community. Also, processing filters for quality control are applied that may remove the worst case waves (Christou and Ewans, 2011), which have been documented, for example, in offshore infrastructure damage. When raw wave recordings are not subject to this filtering treatment, striking examples of the physical dimensions of rogue waves are revealed, such as the wave strike on the *FINO1* research platform in the German Bight during Storm Britta on 1 October 2006 (Herklotz, 2007; Rosenthal and Lehner, 2007; Pleskachevsky et al., 2012; Kettle, 2015). In the absence of digital wave recordings, researchers have taken a different approach to characterize rogue waves by using proxy data, and this has included generating lists of wave strikes on ships and beaches from media reports (Liu, 2007; Nikolkina and Didenkulova, 2012; O'Brien et al., 2013). The present contribution uses a differ-

ent strategy and looks for anomalous patterns in the highest frequency components of tide gauge data during a severe North Sea storm. Many tide gauges are in operation around the North Sea, and the idea is to see if large waves, like the *FINO1* wave during Storm Britta, might generate a meteotsunami or harbour seiche when hitting the coast.

This contribution reviews Storm Daria, which crossed Europe on 25–26 January 1990 causing serious damage onshore and also significant maritime impacts. An overview of the environmental conditions and societal impacts is presented based on reports from the media and scientific literature, and a complete source list is presented in the Supplement. This is followed by a detailed analysis of the storm surge based on tide gauge water levels and possible links with wave events and maritime incidents. The contribution follows similar reports for Storm Anatol in 1999, Storm Britta in 2006, Storms Franz, Kyrill and Tilo in 2007, and Storm Xaver in 2013 (Kettle, 2018, 2019, 2020, 2021, 2023a, b) with modifications and new analysis to take account of the different information available for this earlier storm.

2 Storm Daria and its societal and energy infrastructure impacts

Storm Daria was the first of a sequence of linked storms that travelled across the North Atlantic and into Europe between late January and early March 1990 (McCallum and Norris, 1990). The storm sequence was linked to an unusual surface pressure configuration with a very deep low pressure centre over Iceland and a high pressure centre over the Azores. It resembled the pressure dipole of the North Atlantic Oscillation except it was a persistent synoptic pattern on daily weather maps instead of an average statistical result of a noisy time series (Pinto et al., 2009). The persistent synoptic dipole had never been observed before (Mariners Weather Log, 1990), and record low pressures were measured in Iceland (McCallum and Norris, 1990). Storm Daria had a short, intense life cycle, starting as a shallow low pressure area off the eastern seaboard of North America. The low pressure centre deepened rapidly during its rapid passage across the North Atlantic Ocean and was located off the west coast of Ireland at dawn on 25 January. The low pressure centre passed eastward across the centre of Ireland, then across southern Scotland into the central North Sea where it culminated with a central sea level pressure below 950 hPa in the early evening of 25 January. Its rate of progress was slower after this point as it passed eastward into the Skagerrak north of Denmark and then across southern Sweden into the Baltic Sea. Operational weather forecast systems at the time of the storm were hampered by limitations in the numerical models and the timely availability input measurements (Heming, 1990). Reanalysis weather products only started becoming available in the middle of the 1990s, partly to re-evaluate and understand historic storms, including Storm Daria (Pinto et al., 2009; Roberts et al., 2014; Lockwood et al., 2022). Figures S1.1 and S1.2 show the trajectory and development of the low pressure centre from the PRIMAVERA database of Lockwood et al. (2022), and reveal that the low pressure centre deepened at an average rate exceeding 31 $\mathrm{hPa\,d^{-1}}$, far above the threshold of 24 $\mathrm{hPa\,d^{-1}}$ that characterizes a dangerous meteorological bomb (Sanders and Gyakum, 1980).

Damage during the storm resulted from its incredible wind field. High winds impacted the southwest part of the UK on the morning of 25 January, moving across to London and the southeast in the early afternoon. Very high winds were reported in France in the mid-afternoon (Météo France, 2016). In the Netherlands, the highest winds occurred in the evening rush hour (NRC Handelsblad, 1990b). Figure 1 shows a map of the measured wind speed and direction at 18:00 UTC on 25 January 1990 about the time the central pressure culminated in central North Sea and maximum wind damage was occurring in the Netherlands. In addition to the wind measurements from the meteorological station network, the map shows offshore winds from the passive microwave SSM/I satellite instrument (Wentz et al., 2012), revealing two high wind areas in the southern and northern North Sea on opposite sides of the low pressure centre. Figures S2.1 to S2.15 show wind speed measurements at 3 h intervals across the period of the storm along with other offshore wind speed images from the sun-synchronous SSM/I satellite, which made morning and evening passes over north-western Europe during the period. The images reveal different stages in the storm life cycle, starting with the high wind field southwest of UK on the morning of 25 January (Fig. S2.3). It includes a snapshot of the high wind field in the south-eastern North Sea on the morning of 26 January (Fig. S2.10) when Denmark experienced a storm surge along its west coast and onshore wind damage. Literature from the period emphasized the contribution of visible and infrared satellite images to understand the structure and development of the storm (Mariners Weather Log, 1990; McCallum, 1990; Meteorological Office, 1990). The first wind scatterometers were launched later in the decade, and the important QuikSCAT scatterometer only became available from 1999. The SSM/I passive microwave wind speed measurements were available from 1987, but do not appear to have been used operationally initially. However, later reports emphasized their importance for offshore wind resource assessment as wind farms were being constructed in the North Sea (Hasager et al., 2007a, b).

Radiosonde data give information about the vertical profile structure of wind speed, temperature, and moisture. One month of radiosonde data for stations in Europe (Fig. S3.1) was downloaded from the University of Wyoming (2023) archive for January 1990. Data sections were plotted across the period of the storm. Time series of vertical profiles of wind speed for two stations in the southern UK are shown in Fig. S3.2 for Cambourne and Fig. S3.3 for Crawley. These stations featured in a review analysis of the storm by Hewson and Neu (2015), and they are located at approximately the

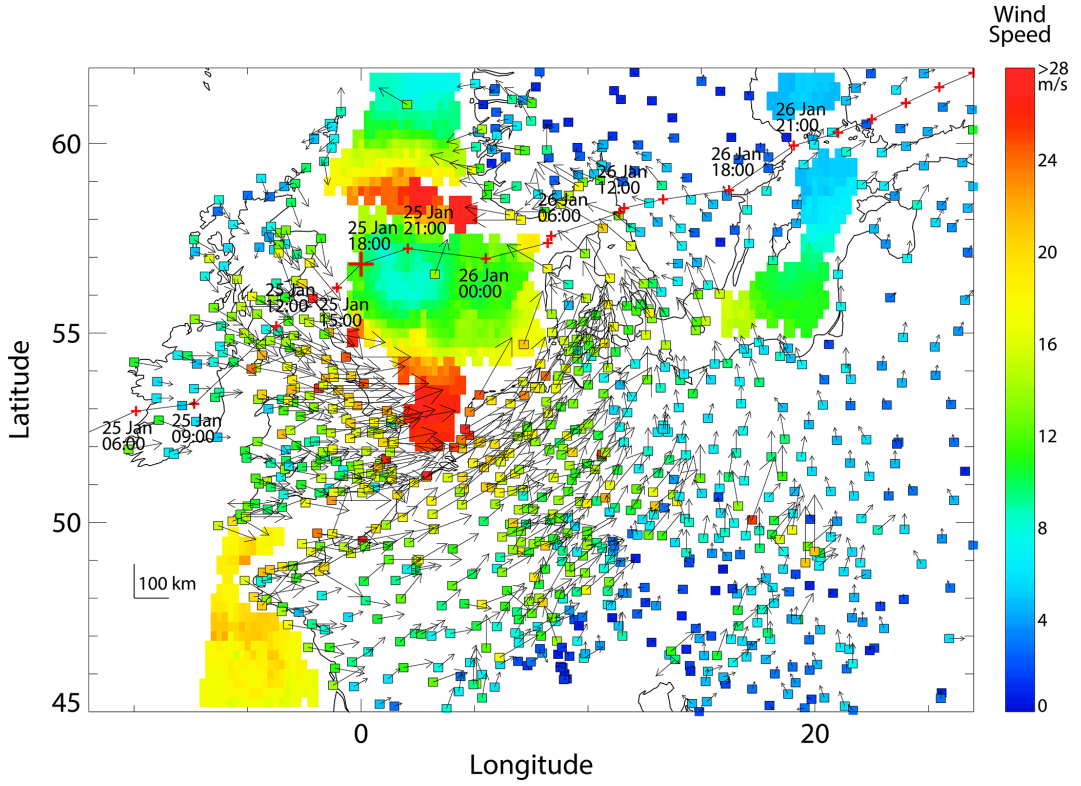

Figure 1. Wind speed and direction for Storm Daria at 18:00 UTC, 25 January 1990 from selected stations of the USAF data set at approximately the time of maximum wind damage in the Netherlands. The trajectory of the low pressure centre is indicated by the black line with red crosses at 3 h intervals (Roberts et al., 2014). The location of the pressure centre at the time of wind field is shown by a larger cross in the North Sea near Scotland. SSM/I sea surface wind speeds (Wentz et al., 2012) are shown for a satellite overpass at about 18:36 UTC or ∼ 36 min after the synoptic station reports. The satellite data indicate suggests that there was a ring of high wind speeds around the low pressure centre at this time, both in the southern North Sea (eastward) and in the northern North Sea (westward).

latitude of highest upper air winds, as revealed in the latitude-height profiles of Figs. S3.4–S3.6. The time series information for these two stations shows that Storm Daria had the highest upper air winds of the month, although there were other storm periods on 17 January, 28 January, and 31 January that were also reported in the media.

Metrics of convective activity were analyzed to understand the origin of the remarkable surface gusts in north-western Europe and the tornadoes that were registered in the Netherlands and Germany (European Severe Weather Database, 2023). Convective Available Potential Energy (CAPE) was extracted from the radiosonde database along with the associated quantities of the level of free convection and the equilibrium level (Johns et al., 1993). Additionally, the severe weather threat (SWEAT) index was extracted (Miller, 1972). These are composite quantities derived from radiosonde profile measurements that give information about thermodynamic stability. They have been used as diagnostic quantities to understand when severe convection and tornadoes may be expected, especially during summer time conditions in the central United States. The physical principles have applicability also to extreme wind regimes in cold climates where high vertical wind shear compensates for the low moisture content of the atmosphere with the potential to generate a winter-time tornado (Johns et al., 1993). Maps of CAPE between 12:00 UTC, 25 January and 12:00 UTC, 26 January are shown in Figs. S3.7–S3.9, highlighting positive values around the North Sea area that increase during the 24 h interval. The values of CAPE are low, but the positive value threshold must be reached for tornadoes to occur, and the recorded tornado cases during the storm occurred near stations registering positive CAPE values. The SWEAT index, shown in maps in Figs. S3.10–S3.12, incorporates metrics of vertical wind shear, and reveals that the tornado threat in northwest Europe during Storm Daria was comparable with the atmospheric state during bad summertime tornado situations in the central US. However, unlike the deep convection systems linked with summer-time tornado outbreaks, the values of the level of free convection and equilibrium level during Storm Daria (shown in Figs. S3.2–S3.9) reveal that atmospheric convection in the areas around the North Sea was actually quite shallow. The *Forschungsplattform Nordsee* far offshore in the southern North Sea was in operation from 1976–1993 (Dolezalek, 1992), and it gives a vantage point

of what was happening in the lower atmosphere over the sea surface during the storm. The time series data in Fig. S4.1 reveal that the high storm winds occurred with a shallow broken cloud field, possibly linked to convection cells forced by high sea surface temperatures in an unstable boundary layer.

The winds from Storm Daria generated a high wave field in the North Sea and particularly in the Atlantic Ocean west and southwest of the UK. Some wave recorders were in operation in the North Sea in 1990 (Figs. S5.1 and S5.2), although they were not as numerous as they would become later in the decade, and technical solutions were still being developed to permit long offshore deployments (Joosten, 2013). The time series data for significant wave height in the North Sea for January and February 1990 are shown in Fig. S5.3. The data reveal that Storm Daria was one of two significant offshore storms during the period, and that Storm Vivian at the end of February was comparable in strength. The wave field for severe European winter storms is often registered at seismic stations through action of waves breaking at or near the coasts. The strength of the associated seismic noise signal depends on different factors, including the distance of the storm, and Storm Daria was noted to have an unexpectedly low signature in a seismic listening station in north Wales (Darbyshire, 1998). Several minor earthquakes were registered in the UK during the 2 d period of the storm with the strongest at 13:42 UTC on 26 January at the island of Colonsay off the west coast of Scotland (British Geological Survey, 2024).

The wave field contributed to significant erosion at certain locations along North Sea coast. Coastal cutback was reported along sections of the Netherlands coast (RWS, 1990; Dorland et al., 1999). On the German coast, a dyke was damaged, forcing the evacuation of the village of Dagebüll (Landesregierung Schleswig-Holstein, 2023), and coastal flooding was also reported in Denmark (Lloyds Weekly Casualty Returns, 1990a). There were literature reports of large land losses from the island of Sylt (Deutschen Wetterdienst, 1990; Franke, 1990), and coastal survey data across the storm period in the first three months of 1990 reveals over 100 m of coastal cutback from the southern tip of the island (Fig. S6.1).

The wave field was also dangerous for shipping, and a series of maritime accidents occurred in north-western Europe with particularly serious cases off the Atlantic coasts of France and the UK. Figure S7.1 shows the locations of offshore shipping events from reports in Lloyds Weekly Casualty Returns (1990a, b) with additional information in Mariners Weather Log (1990) and newspaper reports. The *Celtic Navigator* experienced a shift of its deck cargo of timber off Lands End, leading to a 40° list that was eventually corrected by jettisoning the deck cargo. In the northern Bay of Biscay, the *Iran Abad* also experienced a cargo shift of steel and manufactured products that caused hull damage and required the vessel to take shelter in Brest. In the same area, *Rio Santa Rosa* experienced similar damage when a spare anchor broke loose and was lost overboard. Nearby, the container vessel *ACT 7* lost three containers overboard. Further south in the Bay of Biscay, the *Boqueron* experienced a cargo shift and leak from a large swell. This necessitated a crew evacuation and the grounding of the vessel near Cape Quintres on the Spanish coast (Wubs and Waaldijk, 1990). The sea state was bad, but there are indications that some of the shipping damage in the Atlantic sector was due to rogue wave strikes causing window damage. The wooden trawler *La Fayette* sent a radio report of a broken porthole before vanishing with its crew of five, and the *Santyand* reported a broken bridge window with saltwater damage to its radio and navigation systems. Fatalities were reported with the capsize of the catamaran sloop *Revolution* off Granville in the western English Channel and *Jotun* in the western Baltic. In the eastern section of the English Channel, the *River Adada* experienced steering problems. In the North Sea, the highest profile incident in the newspapers was a machinery breakdown of the Soviet cargo vessel *Briz* off the Netherlands coast, leading to the evacuation of its large crew. Also in the southern North Sea, the harbour tug *Impulsion* capsized off Lowestoft after being hit by the disabled ship that it was towing during storm winds, and *Dover Star* lost its steering. Further north, the platform *Hunter* parted its tow wire to the tug *Viking Troll* and started drifting, and the support vessel *Sea Girl* reported steering problems nearby.

Storm Daria also had notable societal and economic impacts, and Fig. 2 outlines the energy interruptions. There were widespread electrical power outages in the UK, northern France, the Netherlands, Belgium, and West Germany, due mostly to power lines blown down but also to collapsed masts in some places. In the UK, a million customers were reported to have lost electrical power at the height of the storm in a band across southern England and Wales from Cornwall to Kent (Herald Express, 1990). Southwestern England was particularly badly hit, and SWEB News (1990) reported that a maximum of 400 000 customers (or 30 % of the total) were off grid during the first day. The full network damage took about a week to repair even with extra workers flown in from other parts of the UK and support from military units, and field work was complicated by additional storm events. Large scale power cuts were also reported in northern France for hundreds of thousands of people (Belfast Telegraph, 1990; Lloyds Weekly Casualty Returns, 1990b). In Belgium normal electricity distribution was cut by at least 10 % because of broken power lines (Lloyds Weekly Casualty Returns, 1990a). In Denmark, some power outages were registered in southern Jutland in Denmark (Lloyds Weekly Casualty Returns, 1990a), but large scale electrical blackouts did not occur as would be the case during Storm Anatol on 3 December 1999 and Storm Erwin on 8 January 2005 (Danish Energy Agency, 2016). Nuclear stations were impacted during Storm Daria, with a collapsed cooling tower at Paleul on the French Channel coast (Milwauki Journal, 1990; NRC Handelsblad, 1990a), and well as power supply interruptions

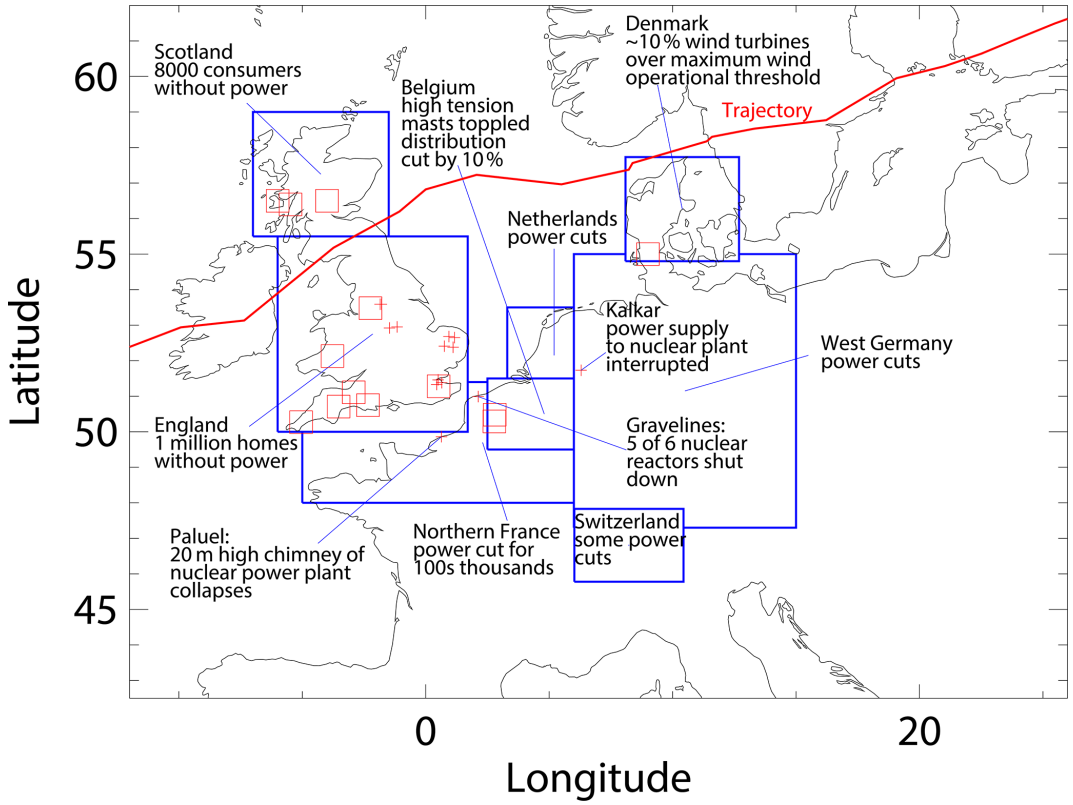

Figure 2. Thematic map of power outages, energy infrastructure damage, and wind turbine incidents that were reported in the literature for Storm Daria 25–26 January 1990. The trajectory of the low pressure centre is given by the thick red line. Blue boxes delimit countries and larger regions with a printed summary of energy impacts. Red boxes smaller regions (English counties, French departements, etc.) with energy impacts. Three cases of problems at nuclear power plants are also indicated.

at Gravelines in France and at Kalkar in Germany (Wetteronline, 2022). About 10 % of the ∼ 2700 wind turbines in Denmark experienced some sort of interruption during the storm. This was mostly reported as production losses as wind speeds crossed the 25 m s^{-1} shutdown threshold (Grøning et al., 1990), but there were also cases of machinery damage including complete turbine destruction (Jensen and Winther-Jensen, 1990; see also Fig. S9.1). Heipertz and Nickel (2008) reported that natural gas production was impaired, and a gas drilling tower collapsed in West Germany (Lloyds Weekly Casualty Returns, 1990a).

In addition to energy supply and distribution networks, the storm had major impacts on transport infrastructure, the built environment, and forestry. These are summarized in Sect. S8 with a series of thematic maps. Figure S8.2 outlines flight diversions and airport interruptions. At Lulsgate airport in Bristol a mid-sized passenger transport aircraft was flipped onto its back, and at Heathrow airport a Boeing 747 jumbo jet was pushed off a taxi way by the strength of the wind. Figure S8.3 shows interruptions to ferry services during the storm, with impacts to services across the Irish Sea, English Channel, North Sea, and Baltic Sea. Some of the interruptions arose from serious offshore events with a case where a ferry (*Chartres*) lost power in the English Channel and incurred further damage while docking in Dieppe. The North Sea ferry *St. Nicolas*, which set out from Harwich for Hoek van Holland, had to return to its port of origin after weathering the storm at sea for 10 h. The ferry from Hamburg to Harwich waited out the storm for 24 h off the Essex coast. Figure S8.4 presents some of the impacts to the railway systems, highlighting severe disruptions in England as almost all London train stations were closed, as well as the almost complete shutdown of the Netherlands rail system. Figure S8.5 outlines some of the road transport interruptions, and there were a number of motorways in southern England, Belgium, and the Netherlands closed by the overturning of high-sided transport vehicles, often with multiple instances on a given roadway. There were numerous cases of small roads across southern England closed by fallen trees, and the traffic situation in London was particularly bad with bridges across the Thames closed. In Scotland and Northern Ireland, different road problems were encountered with blockages due to snow accumulations. Figure S8.6 displays some of the building damage during the storm winds, with media emphasis on high profile cases like de-roofed train stations and sports stadiums, damaged airport buildings, a church tower collapse,

and large-scale destruction of commercial greenhouses in the Netherlands. Radio and television masts were blown down in some areas, affecting communications, and there were multiple reports of toppled cranes. Figure S8.7 shows forest damage across the storm period in the first three months of 1990 from the tabulated lists of Gardiner (2010a). The multiple storms during the period caused damage across western and central Europe, but each storm had a different regional impact, and Storm Daria would have been responsible for the greatest forest damage in the UK, Belgium, the Netherlands, and Denmark. For intercomparison and damage assessment, the industry reports forest damage as a fraction of its growing stock or its annual harvest, and the UK had windfall losses that reached 75 % of the annual harvest. In the Netherlands, windfall losses were lower at 23 % of the annual harvest. This had significant follow-on impacts for fluctuating prices on the timber markets as the damage was cleared (Dorland et al., 1999), and timber market depressions were also noted for Germany and Switzerland (Gardiner, 2010b). Figure S8.8 shows a map of the fatalities and some of the injuries that occurred during the storm. The fatalities were mostly due to traffic accidents linked with trees blown over in the strong winds, and the map highlights how the events were clustered in a narrow band across southern England, Belgium and the Netherlands. In the UK, numerical weather prediction models had forecast the storm 5 d in advance (McCallum, 1990), but the large number of fatalities occurred because the storm hit during a working day (Buller, 1993).

3 Methods

Tide gauge data from stations around the North Sea are analysed to trace the progress of water level fluctuations on different time scales, ranging from the tide to the longer period storm surge and short period seiches. High resolution tide gauge water level data in the North Sea will typically contain a number frequency components comprising a dominant semi-diurnal tide ($\sim$ 12 h), a longer period surge component (on the order of days), and a shorter period seiche component (on the order of minutes or 10s of minutes). The tide must be modelled and subtracted from the measured water level time series to isolate the surge residual. The surge residual originates from high winds forcing water onto a coast, from the possible effect of a travelling external surge entering the North Sea north of Scotland, and from the rise of water under the storm low pressure area (i.e., inverted barometer effect). Wind waves breaking on the coast can also augment storm surge water levels (US Army Corps of Engineers, 1984; Pugh, 1987). Likewise, meteotsunamis (Monserrat et al., 2006; RWS, 2014; Pattiaratchi and Wijeratne, 2015) and harbor seiches (Pugh, 1987; de Jong and Battjes, 2004) may be important in the short period component of tide gauge data in certain instances.

Tide gauge data sets were obtained from the national monitoring agencies for countries around the North Sea. Most data were downloaded from online Internet sites for the UK (BODC, 2024), the Netherlands (RWS, 2024), Denmark (Kystdirektoratet, 2024), and Norway (Kartverket, 2024). Data sets for Belgium, Germany, and two stations in Denmark were obtained by email contacts. Studies of older storm surge events have identified a problem of lost data archives (Wadey et al., 2015), but 1990 was within the recent period when digital archives were available. A strategy was adopted to obtain data from all possible water level measurements for January 1990 showing a tidal signal, and then perform a preliminary analysis to eliminate time series that were malfunctioning or had extended data gaps. A few stations for Denmark had short data gaps, and these were linearly interpolated. The Havneby station had the worst data gap of 5 h on the afternoon of 26 January 1990. The source and key characteristics for the data sets are shown in Table S10.1. Table S10.2 shows a list of stations that were rejected because they showed unusual trends or had extended data gaps, and several stations in Denmark (Esbjerg, Ribe, Thorsminde Havet) failed near the height of the storm surge. Altogether, 103 stations were used in the analysis after the quality control steps, and these are shown in the maps of Figs. 3 and 4. There was a high spatial density of stations, particularly along the coasts of the Netherlands and Germany.

For the high resolution tide gauge time series of the UK, the Netherlands, Denmark, and Norway, data preparation is the same as for previous storm studies (Kettle, 2018, 2019, 2020, 2021, 2023a, b). A 16 d data segment from 14–29 January 1990 (inclusive) was extracted from the longer source data files with the dates chosen to include the 2 d period of Storm Daria 25–26 January 1990, plus an earlier storm on 18 January 1990 that was mentioned in the literature for the North Sea *Ekofisk* platform (Rambøll, 1999). The data discretization for the different national authorities was either 10 min for the Netherlands and Norway, 15 and 30 min for Denmark, or 60 min for the UK and the German station of Cuxhaven. A discrete Fourier transform was conducted to translate the time series data for a single station into the spectral domain (Stull, 1988; Gönnert et al., 2004). The spectral plot was inspected visually to assess the frequency thresholds for the different water level components: long period (mostly storm surge), short period (mostly harbour seiche or meteotsunami), and tidal (diurnal plus semidiurnal, combined). Figure S11.1 graphically shows the frequency thresholds that were used to define the spectral components for a sample station at Delfzijl in the northern Netherlands; the same thresholds were used for all the stations. The 0.2 d (or 4.8 h) threshold was chosen to separate the long-period and short-period reconstructions, and this is similar to previous studies that have aimed to isolate meteotsunami signals in water level data showing a strong tidal component (Monserrat et al., 2006; Pattiaratchi and Wijeratne, 2015; Zemunik et al., 2021). For the present study, caution should be exercised

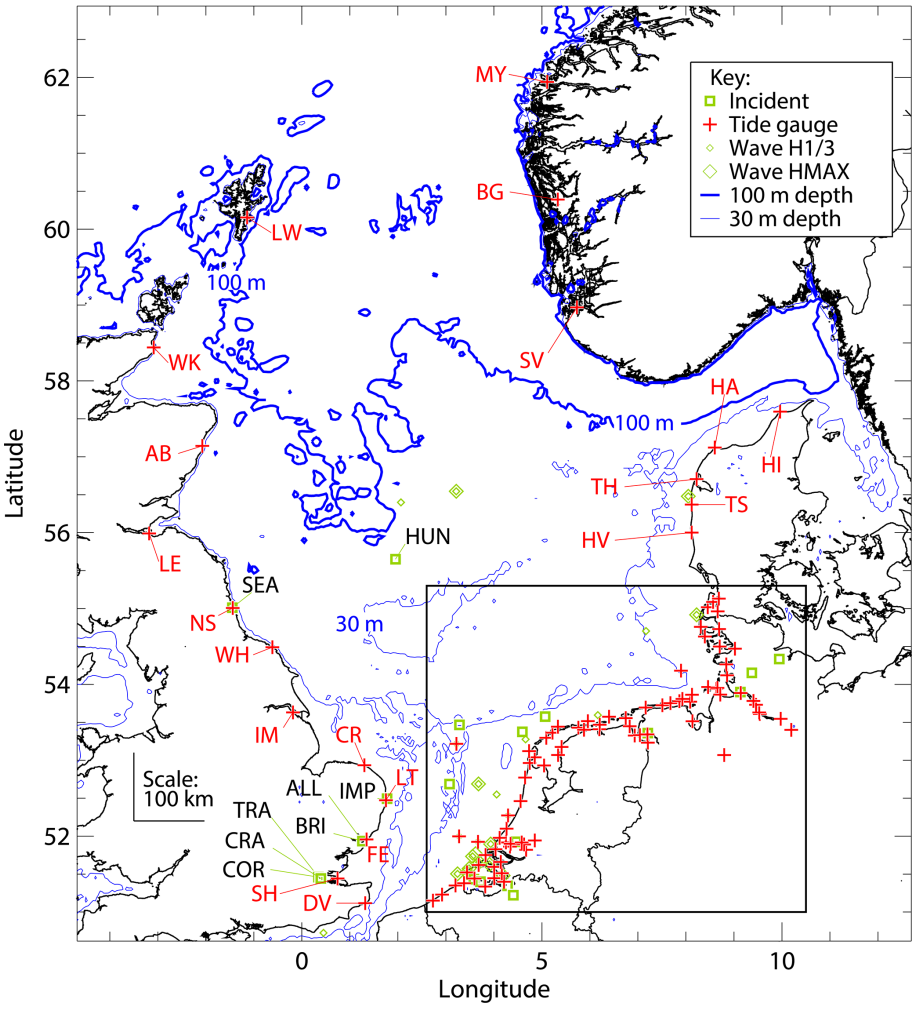

Figure 3. Location of tide gauges analyzed in this study and of North Sea maritime incidents that were reported over the 2 d period 25–26 January 1990. For presentation clarity, the information in the inset box covering the south-eastern North Sea is shown in Fig. 4. The abbreviation codes for the tide gauges and maritime incidents are explained in Tables S10.1 and S13.1.

in interpreting time series with the longer time discretizations of 1 h, as meteotsunami signals would not be clearly resolved.

The spectral analysis procedure had to be modified for the data from Belgium and Germany (except for Cuxhaven) because high resolution data (i.e., 1–60 min recording intervals) were not available. National sea level monitoring agencies over the past half century have responded to technological advances in instrumentation and data storage by increasing the temporal resolution of water level data. In the pre-digital period, time series of tide gauge data were archived at lower resolution, consisting of sequential series of high and low water levels (i.e., data at approximately 6 h intervals), which was about the limit of what could be processed by hand for summary statistics. Germany and Belgium were still using this protocol in 1990, and Germany only shifted to higher resolution recordings late in the 1990s. The tide gauge analysis for Storm Daria thus had to accommodate these lower resolution data sets, in addition to the normal higher resolution time series available since the late 1990s. The low resolution time series data from the North Sea have a saw tooth pattern from the dominant semidiurnal tide, but are modulated on longer time scales by storm surge effects and also monthly/semi-monthly tides. Closer examination of the data reveals that the two daily tidal peaks are not the same because of additional effect of the diurnal tide. It was not possible to isolate a short period component (i.e., < 4.8 h) from these coarse resolution data. The challenge was rather to separate the multi-day surge signal from the shorter period semidiurnal and diurnal tides, and the longer period semi-monthly and monthly signals. The strategy to achieve this was to conduct the same discrete Fourier transform analysis as for the high resolution data but to use different spectral cut-off frequencies to remove the semidiurnal and diurnal tides (i.e., periods < 1.2 d) and semi-monthly and monthly tides (i.e., periods > 12 d), leaving the storm surge signal in the spectral

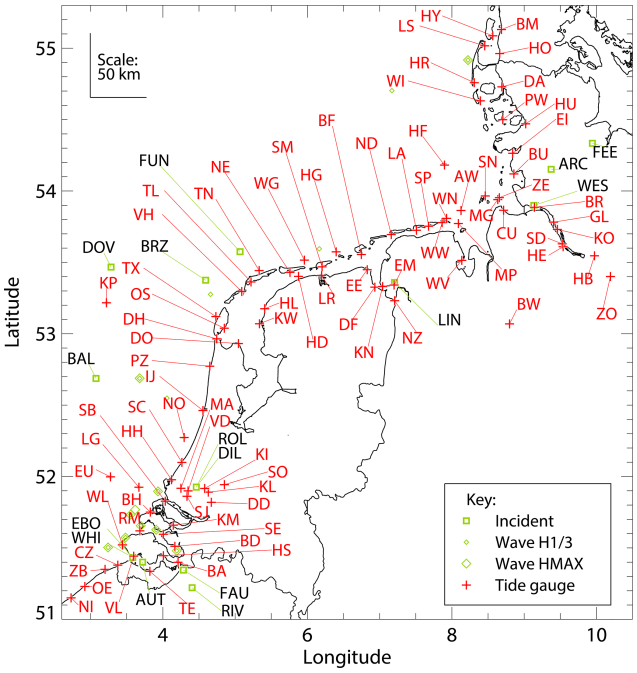

Figure 4. Location of tide gauges and maritime incidents along the North Sea coasts of Belgium, the Netherlands, Germany, and southern Denmark. The abbreviation codes for the tide gauges and maritime incidents are explained in Tables S10.1 and S13.1.

gap of 1.2 to 12 d. The analysis assumes that the data were regularly spaced in time, which was approximately true for these data. The low temporal resolution of the data permitted longer time series to be used with the discrete Fourier analysis. The full length of the available data sets were used in the analysis, which was 3 months for Germany and 12 months for Belgium.

There is a potential tide gauge levelling problem that was identified in Kettle (2021, 2023a, b). It originates from the observation that the average levels of most of the downloaded data sets (except for Belgium) were a few tens of centimetres above the official sea levels, and could not be resolved with the water level variations expected on a monthly or seasonal basis (Fig. S12.1). The pattern of offsets observed for Storm Daria in 1990 is similar to the analysis of storms after 1999, but the sea levels in 1990 were 5–10 cm lower than in 2007 (Kettle, 2023b), for example. To make the sea level data from this analysis comparable with literature reports, values of skew surge and true surge are adjusted upward by the amount of their apparent sea level inconsistency. Figures S12.2 and S12.3 illustrate the impact of these corrections for the maximum true surge and skew surge in comparison with literature values.

A short database of maritime incidents in the North Sea area was compiled (Table S13.1) to compare with the largest oscillations in the short period reconstruction of the water level time series. These were gathered mostly from Lloyd's Weekly Casualty Returns (1990a, b), and supplemented with reports from Mariners Weather Log (1990). Some of the offshore incidents have been outlined above, but there were also many cases of mooring line or anchor failures in or near ports, as well as insurance team inspections in the days following the storm. Storm damage was identified or implied, but these other reports typically did not have much time information, sometimes not even a date. In addition to the maritime accident reports, information was drawn from the time series of wave statistics available in the North Sea area. Although there were not as many wave records available in 1990, a significant number of time series records were gathered mostly from the southern North Sea (Fig. S5.2). Most of these were part of a network operated by Rijkswaterstaat off the coast of the Netherlands, but other national agencies often had at least one in operation. Information for the time of maximum values of significant and maximum wave height during the 2 d period of the storm were extracted and appended to list of shipping incidents for comparison with features in the tide gauge data. Kettle (2023b) presents more information about the features of North Sea wave data.

4 Results

An overview of the results is shown in Fig. 5 as a cascade diagram of time series for the tide gauge stations around the North Sea. The first panel (Fig. 5a) of the diagram shows the original data as received from source authorities after being detrended with a straight line. The subsequent panels show the water level information divided according to the different time scales from the spectral separation procedure: long period component (Fig. 5b), tidal component (diurnal plus semidiurnal; Fig. 5c), and high frequency component (Fig. 5d).

In presenting the time series data, the tide gauge stations are arranged counter-clockwise around the North Sea starting with Lerwick in Scotland at the top and ending with Maløy in Norway at the bottom. It contrasts with the meteorological convention of presenting storm spatio-temporal information along the path of westerly winds or the low pressure trajectory. The different presentation convention for storm surges was established in the earliest North Sea investigations from the late 1940s (Corkan, 1950). The tides in the North Sea travel counter-clockwise around the basin as coastally-trapped Kelvin waves, entering the North Sea north of Scotland. The surges for certain storms also follow this behaviour, and these external surges have the potential to augment coastal surge flooding. Because storm surge flooding is dependent on the state of the tide, instrumental water level recordings are arranged according to counter-clockwise placement around the basin, and this forms a type of diagnostic to understand water level dynamics during the storm. Because the tidal propagation speed along the shoreline is approximately constant around the North Sea, it permits a fur-

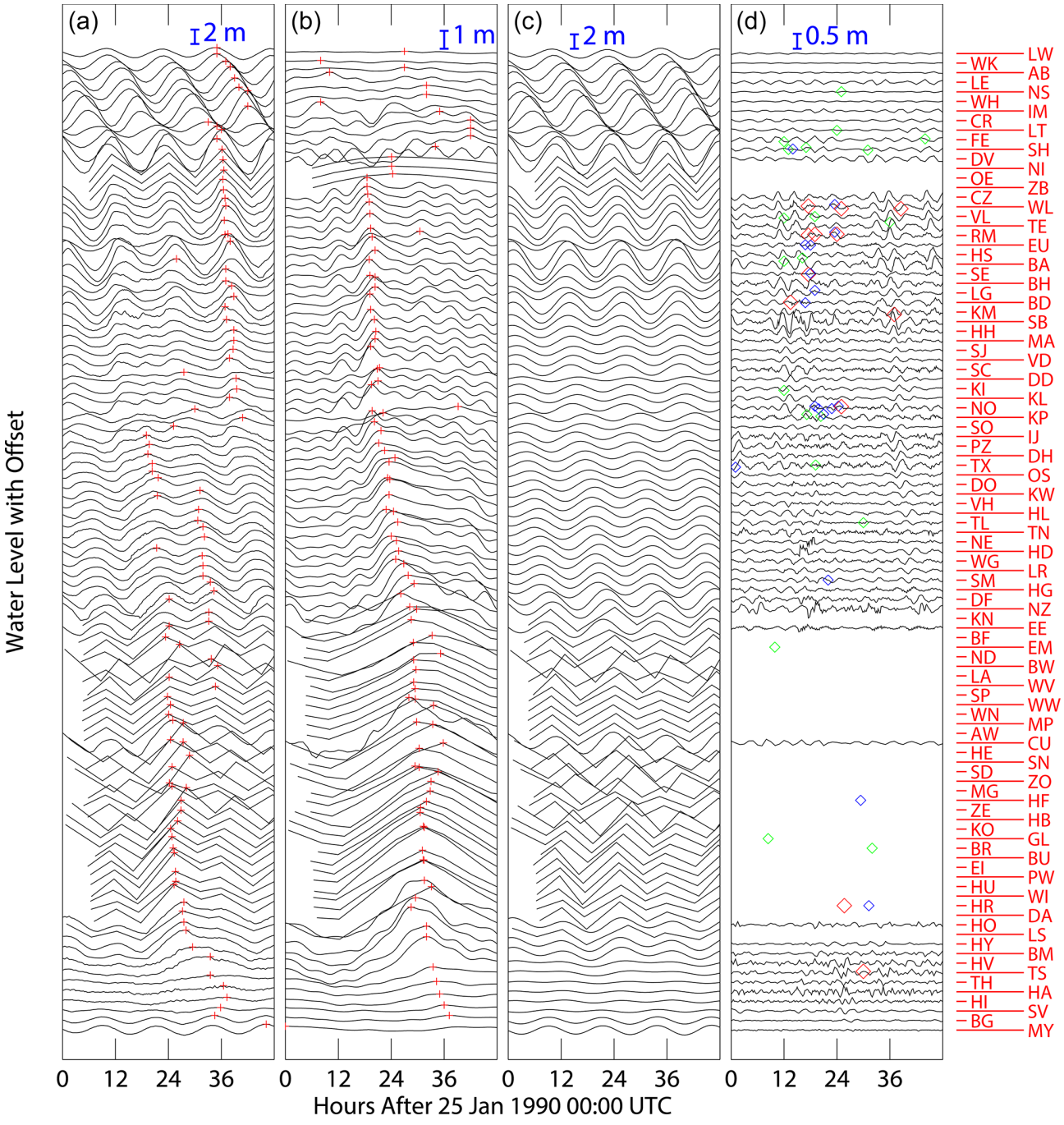

Figure 5. Time series of the **(a)** original water level data, and reconstructions of the **(b)** long period, **(c)** diurnal plus semi-diurnal tide, and **(d)** short period components of the original time series. The station identifications are given by two letter codes along the right hand side of the fourth panel. The stations have been vertically offset according to their relative arrangement counter-clockwise around the North Sea, starting from Lerwick in Scotland at the top and ending with Maløy in Norway at the bottom. In the first two panels, red vertical crosses indicate the maximum of the data segment shown. In the last panel, diamonds mark the time of events at the closest tide gauge station: green for maritime incidents, blue for maximum significant wave height and red for maximum wave height.

ther quantification of the diagnostic, which is explored further below.

Presenting station data in this manner allows the fluctuation features in the time series in Fig. 5a to be followed from one station to the next, with forward offsets in time. The highest levels of each series are shown by red plus symbols, and these assist in tracking the progression of water level features. The most prominent features in the source data are

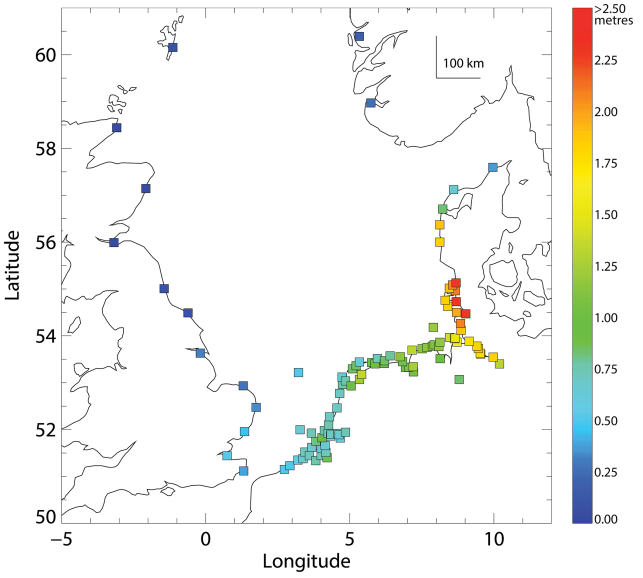

Figure 6. Map of skew surge for tide gauge stations around the North Sea during Storm Daria 25–26 January 1990.

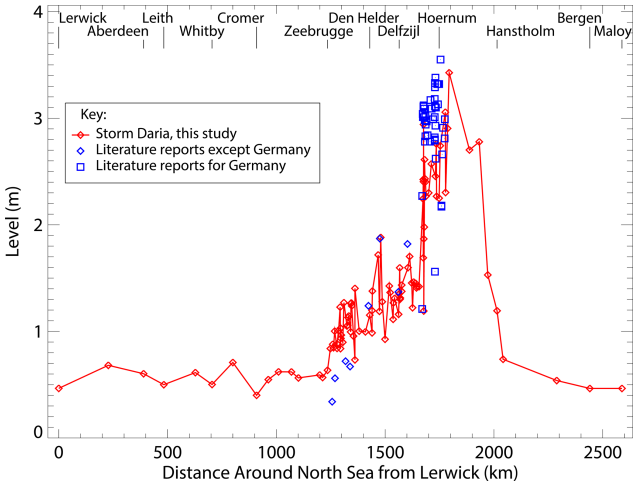

Figure 7. Skew surge during storm Storm Daria on 25–26 January 1990. The values are calculated from tide gauge records and arranged by counter-clockwise distance around the North Sea starting from Lerwick in Scotland. Literature reports are included for comparison. Note that the skew surge convention for German sources is to subtract the measured maximum water level from the long term average high tide level.

the repeated peaks of the semi-diurnal tide, at intervals approximately every 12 h. The tidal signal is shown isolated in Fig. 5c. The 12 h repeat time is shown clearly, even in the low resolution data sets of Belgium and Germany, where it appears with a saw-tooth pattern. The panel also highlights how the tidal amplitude varies at different locations around the North Sea with eastern England and the German Bight having a high tidal range, and northern Denmark having a low tidal range. For the storm surge warning services of the Netherlands and Germany, for example, the coastal flooding potential is closely linked to the times of the high tide (Jensen and Müller-Navarra, 2008).

The storm surge signal in Fig. 5b appears clearly when the tide is spectrally removed from the source data. Stations especially in the southern and western parts of the North Sea show the broad peak of the storm surge wave with a duration on the order of 1 d (RWS, 2014; Gönnert and Buß, 2009). Stations along the coast of the Netherlands show a sharp rise initially followed by a slower decrease of the water level. Water levels for tide gauge stations in the German Bight and the southern part of the Danish west coast indicate that the rates of water level rise and decrease were about the same. (Surge patterns for the German tide gauge stations could be resolved in spite of the low temporal resolution of the source data sets). Following the red plus symbols on the time series curves, the progression of the surge peak can be followed from one station to the next, moving north-eastward along coast of the Netherlands, Germany, and finally Denmark. The highest surge water levels were in the eastern part of German Bight and southern part of west coast of Denmark, where some coastal flooding was reported. In the northern part of Danish west coast the surge level was negligible. Likewise, along the east coast of Scotland and England, the strong winds were mostly offshore, and high surge levels did not develop.

The spatial distribution of maximum water level during the storm is shown in Fig. 6 as a map of the skew surge around the North Sea. The skew surge is calculated as the difference between the measured water level and nearest high tide. It is a measure of the height that the water level attained over the expected high tide level. It is a more effective representation of the coastal flooding threat than the surge residual shown in Fig. 5b, since a surge maximum can occur at tidal low water and not represent a flooding threat. In Fig. 6, the highest skew surge occurred along the North Sea coast of Schleswig-Holstein in Germany and southern Jutland in Denmark with maximum levels that exceeded 2.5 m at certain stations. Skew surge levels along the coast of the Netherlands were lower, and ranged from under 0.6 m in the south to about 1.2 m in the north. Skew surge levels along the coasts of eastern Scotland and England were all lower than 1 m. Likewise, skew surge levels in northern Denmark and Norway, were also lower than 1 m, and these areas were on the north side of the low pressure trajectory. There is agreement with the literature reports of the skew surge levels (Figs. 7, S12.3) after a correction is made to account for differences in mean sea level on a station by station basis (Fig. S12.1).

In coastal engineering studies, storm surge water level reports are difficult to assess in isolation, unless they are placed in the context of water levels from past storms. This especially true in the North Sea where different coastal regions have different tidal range characteristics, and also different

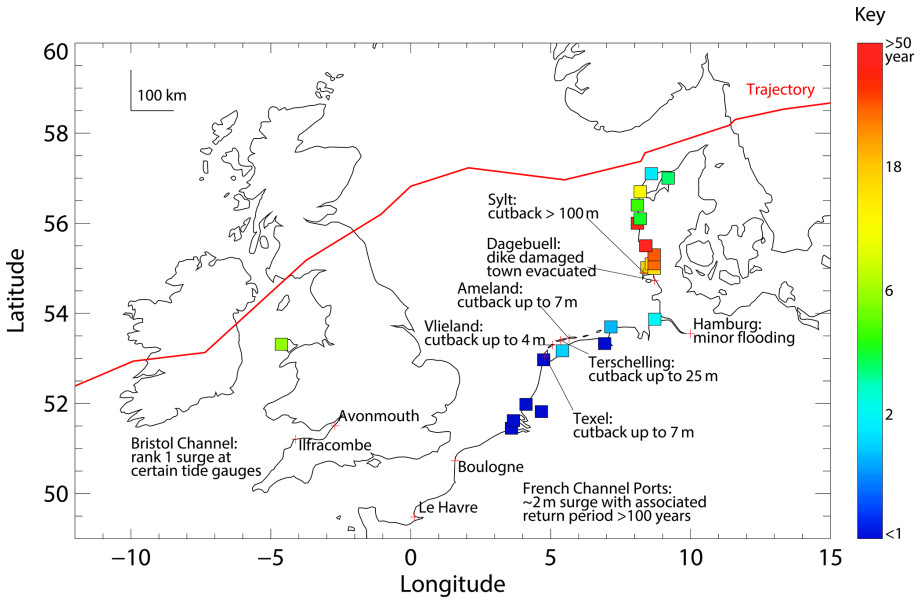

Figure 8. Return period of maximum water level during Storm Daria on 25–26 January 1990, as calculated from literature summary results. There are literature reports of high water levels at certain tide gauges in the Bristol Channel (Gao, 2017) and along the French Channel coast (Météo France, 2016). The associated return periods for these locations are not given in the original sources, but information in Simon (2008) suggests that the return periods for water levels along the French Channel coast may have been high. Cases of coastal damage and flooding along the North Sea are also labelled.

characteristic surge levels during historic storms. Coastal engineering structures take these differences into account, and there is only a flooding threat if a storm surge water level greatly exceeds historic values. One way to assess the seriousness of a storm water level at a particular location is to give it a rank with respect to previous storm levels, and many national monitoring authorities generate ranked storm surge lists (Ditlevsen et al., 2018; RWS, 1990; NTSLF, 2024). This gives an accurate idea of seriousness of a storm surge for tide gauges with long data records, but is less good for newer tide gauge stations that may not include important storms of the 20th century. Ranked storm surge lists can be used to work out the return period of the exceedances of storm surge water levels. For less serious storms, this can be calculated as the ratio of the measurement time interval divided by the number of storm urges above a threshold level. For more serious storms where the coastal flooding levels are unprecedented, statistical extrapolation methods are used to work out the return period (Ditlevsen et al., 2018). The return periods of the water levels for Storm Daria are shown in Fig. 8 on a regional map, and Supplement Table S15.1 gives information on the literature source material. Several stations in southern Denmark had water levels that reached the level of a 50 year return period event (Hvide Sand, Esbjerg, and Thorsminde). The German station of List near the Danish border also registered a high return period of about 20 years, consistent with the coastal cutback damage at Sylt outlined above. For stations along the coast of the Netherlands, the storm surge event was less serious with return periods of a couple of years or less, but some coastal damage still occurred. For the UK, the return periods of water levels for stations along the North Sea coast were not high. However, on the west coast of the UK, the strong winds were blowing onshore, and the highest water level at Holyhead in Wales exceeded the level of a 5 year event. Several stations were highlighted in the literature for unusually high surge levels (Avonmouth and Ilfracombe in the Bristol Channel; Gao, 2017) or skew surge levels (Le Havre and Boulogne in the English Channel; Météo France, 2016). The associated return periods were not presented, but they may have been significant, especially for the cases along the French coast (Simon, 2008).

Time series of the short period component of the water level signal are shown in Fig. 5d. The low resolution data sets for Belgium and Germany could not be used here, and even the 1 h time series data for the United Kingdom and German station of Cuxhaven should be interpreted with caution as they would not have been able to capture short period features in the same manner as the 10 min resolution data of the Netherlands, for example. The range of water levels in this panel is small compared with long period (surge) and tidal components, with maximum values on the order of tens of centimetres. However, the panel is presented to identify possible harbour seiches or meteotsunamis that are excited by transient atmospheric phenomena or possibly large waves. In interpreting these time series, it is most important to identify the maximum oscillations, taking account of their time of occurrence, amplitude, and apparent frequency characteristics. For example, the largest amplitude features along the Dutch

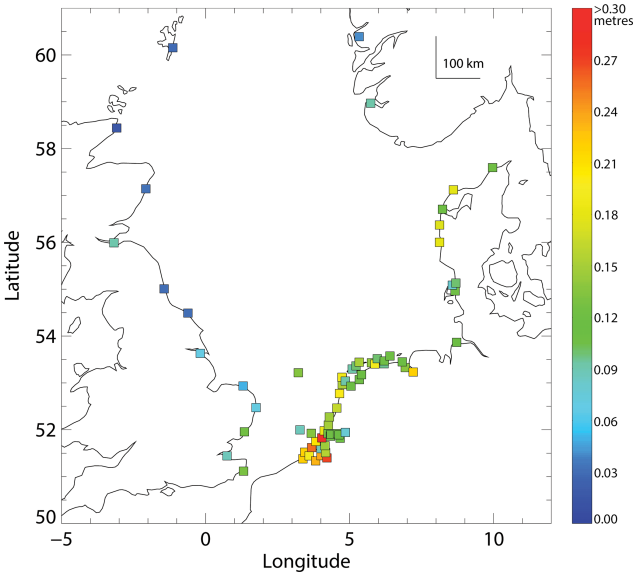

Figure 9. Map of maximum amplitude of highest short period oscillation during Storm Daria on 25–26 January 1990.

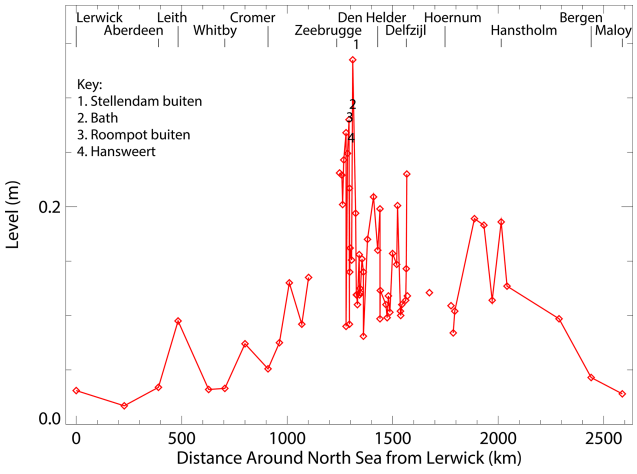

Figure 10. Maximum amplitude of highest short period oscillation during Storm Daria on 25–26 January 1990 versus coastal distance around the North Sea starting from Lerwick in Scotland. Selected outlier stations have been labelled.

coast occur during the early afternoon of 25 January 1990 starting in the southern part of the country near border with Belgium. It comprises a set of 2–3 successive oscillations with a characteristic period in the range 3–4 h (see also Tables S16.1 and S16.2), which is in the approximate range of the higher level tidal harmonics. The short period feature occurs just before the surge maximum and appears to travel north-eastward along the coast like the surge, and its progression can be traced from station to station. A second set of oscillations with comparable characteristics appears on 26 January 1990 just before noon, also travelling north-eastward along the coast. These features are not clearly visible along the west coast of Denmark, and the oscillations here have small amplitudes and shorter period features < 2 h, so they might not be directly linked with the tide.

The spatial distribution of the highest amplitude short period features is shown on a map in Fig. 9 (see also Table S16.2). The largest amplitude features occurred along the southern coast of the Netherlands. Figure 10 shows another projection of this information plotted versus coastal distance around the North Sea, and it emphasizes how the highest amplitude features tended to cluster together on a short section of coast. The spatial pattern contrasts with the maximum surge residual and skew surge, which had their maximum values further to the east in the region of Schleswig-Holstein in Germany and southern Denmark.

The maritime incidents and highest significant and maximum wave heights during the storm are also shown in Fig. 5d, and are plotted on the time series trace of the nearest tide gauge station. Most of the offshore incidents occur on the first day of the storm on 25 January 1990 between noon and early evening. Many incidents are associated with the high oscillation feature about noon that appears in many of the tide gauge stations for the Netherlands. A few events are shown off the coast the Netherlands about noon on 26 January 1990. The short period features from the tide gauge data would not have been responsible for the maritime incidents, having amplitudes extending only to a few decimetres. However, there might have been a passing squall or convection system that might have excited a harbour seiche in the tide gauge data and also caused a maritime incident or perhaps an unusual signal in a wave recording. The possible mechanism for such an meteorological event has been explored by Pleskachevsky et al. (2012) to attempt an explanation of the large *FINO1* wave on 1 November 2006 during Storm Britta.

Figure 11 presents a summary graph that summarizes the spatio-temporal relationship among the different quantities derived from the tide gauge as well as the maritime incidents and waves (see also Sect. S17 for simplified graphs of this information). Plotted on axes of time versus counterclockwise distance around the North Sea, the successive tidal peaks at ~ 12 h intervals appear as diagonal lines as they travel around the basin. The surge maximum has a similar trend as the travelling tide, but the diagonal line showing its progression has a temporal break or offset between the western and eastern sides of the North Sea. There is a coherent travelling surge in the eastern part of the North Sea on 25 January 1990, and this is linked with storm surge flooding in southern Denmark. The maximum surge signal along the east of coast of England appears as an unrelated but coherent event the following day on 26 January 1990. The highest and second highest short period oscillation from the tide gauge analysis are shown as vertical bars the diagram (red and blue, respectively). Along the coast of the Netherlands, they cluster in two groups with one group before the storm surge in the early afternoon of 25 January 1990 and a second

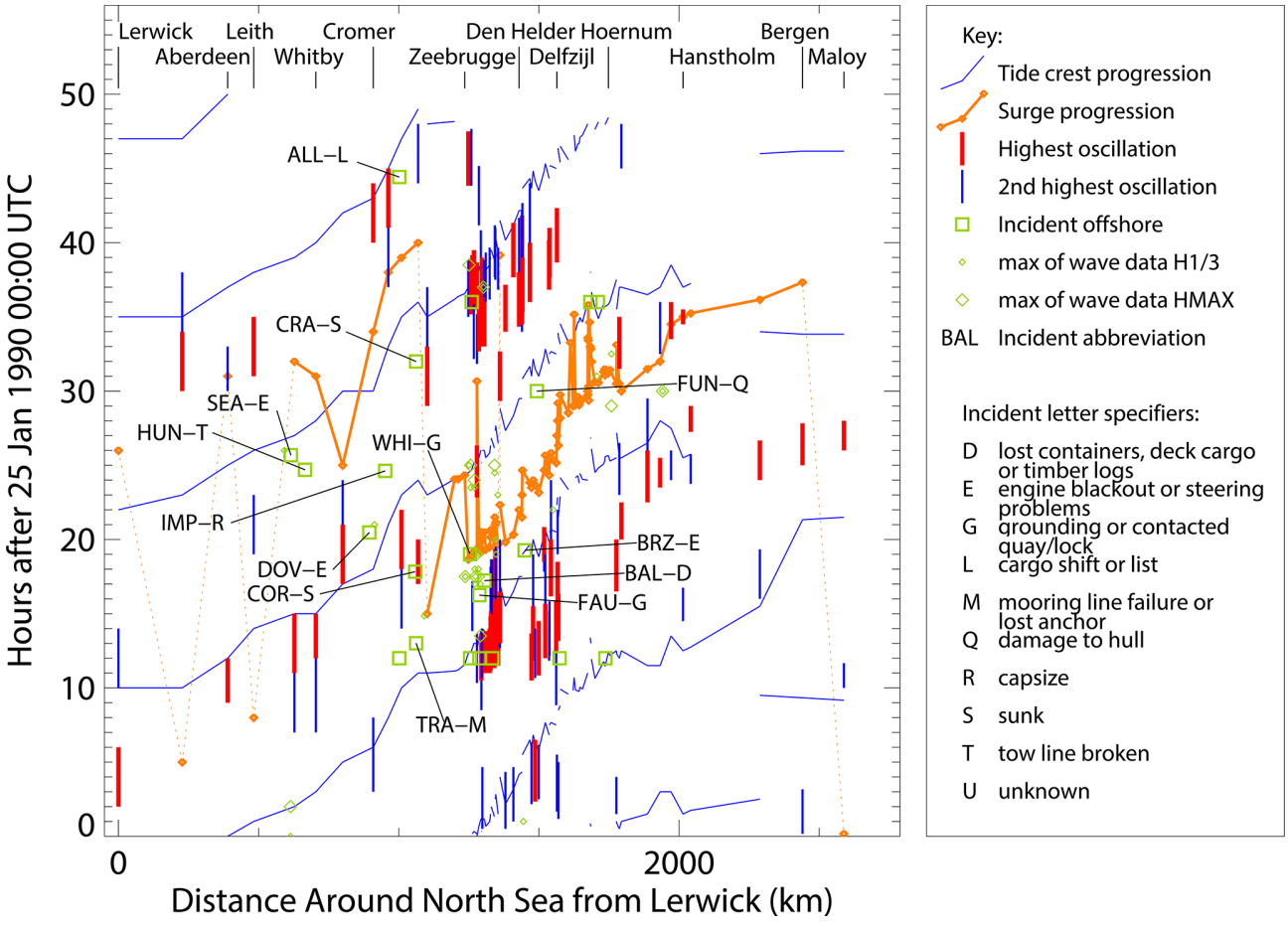

Figure 11. Summary of the progression of the tidal crests and storm surge peak around the North Sea on 25–26 January 1990, and spatial-temporal relationship of peak-to-trough range of the highest up-crossing short period oscillations in the tide gauge record. Maritime incidents/accidents and the highest significant and maximum wave heights from recorders around the North Sea are also indicated. The data are plotted on axes of time versus counter-clockwise distance around the North Sea starting from Lerwick in Scotland. Maritime incidents are labelled with their three letter abbreviation if the uncertainty in the time of the event is less than 12 h.

group occurring on the following day. The diagonal distribution of these oscillations indicates they are travelling in a similar manner as the tide and surge, as was noted in the interpretation of Fig. 5d. The maritime incidents are plotted on the same set of axis with different symbols used for shipping accidents (squares) and wave records (diamonds). Several maritime incidents occur in association with the surge maximum, including the high profile case of the *Briz* near the Dutch coast. The possible link between surge peak and maritime incidents may be caused by the interaction of the strong westerly winds with the tidal currents that occur in relation to water levels. Gemmrich et al. (2009) has pointed out that the occurrence of rogue waves in coastal regions along the Pacific coast of Canada may be caused by how wind waves interact with tidal currents, although the phase relation differs among stations. In the North Sea during Storm Xaver in 2013, Parsons and Frampton (2014) and Spencer et al. (2015) noted that the peak significant wave height appears linked to local water levels, but the exact timing relation differs from place to place along the east coast of England. With respect to Fig. 11, examination of case studies from other North Sea storms may help to assess if there is a general association between storm surge peak, tidal levels, and maritime incidents.

5 Conclusions

Storm Daria is ranked among most serious European winter storm events of the last half century in terms of both economic losses and fatalities. There was a lot of damage to power networks and societal infrastructure, and it took several days restore power and transportation systems in the worst instances. Forest damage was cleared over the following months, and the windfall timber disturbed market prices in the Netherlands and other countries over the following year. Wind energy was less impacted by the storm as Denmark was the only country at the time with a large num-

ber of onshore turbines. This would change starting from the early 1990s when other west European countries expanded wind energy, including offshore turbine demonstration projects (Pasqualetti et al., 2004). Reflecting on events in the Netherlands, Dorland et al. (1999) points out that damage from Storm Daria was cleared rapidly and that modern societies are resilient to windstorm events. Heipertz and Nickel (2008) clarify the cost of the storm damage in larger economic terms, pointing out that damage represented on the order of 0.1 % of the annual Gross Domestic Product for most of the impacted countries in north-western Europe and was thus not a significant economic burden.

It is interesting to compare Storm Daria with later winter storm case studies (Kettle, 2018, 2019, 2020, 2021, 2023a, b) from the following years to assess the relative storm impacts and elucidate if the storm severity may have been becoming worse. Storm Daria remains among the top-ranked European winter storms of recent decades for the number of fatalities, although the impact of surge flooding during the 31 January–1 February 1953 storm was over an order of magnitude worse (Steers, 1971; McRobie et al., 2005). The maximum skew surge levels of Storm Daria were significant but impacted a limited area in the eastern North Sea. Higher skew surge water levels were attained during Storm Xaver from December 2013 over a larger section of coast, and these actually exceeded the 1953 levels at some locations (Wadey et al., 2015). However, the flooding damage was much less because of advances in coastal engineering protection levels. In terms of the spatial footprint of severe winds, Storm Kyrill in 2007 was larger than Storm Daria (Roberts et al., 2014). Storm Kyrill also had about three times the number of reported tornadoes, and it spawned a significant derecho that penetrated south-eastward from central Europe possibly as far as Ukraine (Gatzen et al., 2011; Kettle, 2023a). The radiosonde data from Storm Daria are interesting because the maximum upper air wind speeds are much lower than later winter storms like Storm Anatol in 1999 and Storm Kyrill in 2007 (Kettle, 2021, 2023a). The issue of changes in Jet Stream wind speed had been flagged by the report DWD (2000), which identified a step-change increase of maximum upper tropospheric winds for the period 1995–1998, based on an analysis of European radiosonde ascents extending back to the mid-1970s. The implication of a possible climate-linked change in upper atmospheric circulation is important (Slingo, 2019), but the DWD (2000) investigation was never followed up.

Data availability. The water level data for this study were measured by the national tide gauge networks of the UK, Belgium, the Netherlands, Germany, Denmark, and Norway. The data were downloaded from publicly accessible websites maintained by the national authorities for the UK, the Netherlands, Denmark, and Norway. The tide gauge datasets for the German North Sea coast originated from The Federal Waterways and Shipping Administration and communicated by email from Wilfried Wiechmann of the Federal Institute of Hydrology (Bundesanstalt für Gewässerkunde, BfG). Ellen Lenaers of the Vlaams Ministerie van Mobiliteit en Openbare Werken (MOW) of Belgium emailed time series records of high water and low water values for Nieuwpoort, Ostend, and Zeebrugge. Bjørn Frederiksen of Kystdirektoratet in Denmark emailed data for the tide gauge stations of Hanstholm and Hirtshals, which are not available online. Further information on the URL addresses for the online data sets is given in Table S10.1 of the Supplement.

Supplement. The supplement related to this article is available online at: https://doi.org/10.5194/adgeo-65-83-2024-supplement.

Competing interests. The author has declared that there are no competing interests.

Disclaimer. Publisher's note: Copernicus Publications remains neutral with regard to jurisdictional claims made in the text, published maps, institutional affiliations, or any other geographical representation in this paper. While Copernicus Publications makes every effort to include appropriate place names, the final responsibility lies with the authors.

Special issue statement. This article is part of the special issue "European Geosciences Union General Assembly 2024, EGU Division Energy, Resources & Environment (ERE)". It is a result of the EGU General Assembly 2024, Vienna, Austria, 14–19 April 2024.

Acknowledgements. The author gratefully acknowledges data from national tide gauge networks of the UK, Belgium, the Netherlands, Germany, Denmark, and Norway. The tide gauge data for the UK, the Netherlands, Denmark, and Norway was downloaded from Internet servers. For Belgium, Ellen Lenaers of the Vlaams Ministerie van Mobiliteit en Openbare Werken (MOW) emailed time series records of high water and low water values for Nieuwpoort, Ostend, and Zeebrugge for 1990. For Germany, Wilfried Wiechmann of the Bundesanstalt für Gewässerkunde kindly emailed time series data of high water and low water values for the North Sea stations of Germany. Bjørn Frederiksen of Kystdirektoratet emailed data for two tide gauge stations (Hanstholm and Hirtshals) in northern Denmark that were not provided on the public Internet server. The following people provided background reports, data, or other information to support this review: Mark Beswick (UK Met Office National Meteorological Archive, UK), Maria Blümel, Hauke Thiesen and Theide-Erk Woeffler (Landesbetrieb für Küstenschutz, Nationalpark, und Meereschutz Schleswig-Holstein, Germany), Jeanine Borst (Royal Netherlands Meteorological Institute), Lisa Clarke and Sean Jones (NOAA Central Library, USA), Ineke Glaser-Muller (Nederlandse Organisatie voor Toegepast Natuurwetenschappelijk Onderzoek), David Hawthorn (British Geological Survey, UK), Christian Sjøstrann Jørgensen (Danish Energy Agency, Denmark), Peter Keitz and Andrea Lehnhardt (Deutsche Meteorologische Bibliothek of the Deutscher Wetterdienst, Germany), Peter

Lamb (Electricity History Society, Bristol, UK), Julia Lockwood (Met Office Hadley Centre, UK), Delila Montes (International Energy Agency), Jos Neelen (Weerspiegel journal, the Netherlands), Irene Perez-Gonzalez (Bundesamt für Seeschifffahrt und Hydrographie, Germany), Reidun Gangstø Skaland (Met.no, Norway), Christina Louise Sørensen (Energimuseet at Bjerringbro, Denmark) and Gerda van Vliet (Koninklijke Nederlandse Redding Maatschappij, the Netherlands). The manuscript was improved by the comments of two reviewers. The funding support provided by editor Sonja Martens for the publication costs was greatly appreciated.

Review statement. This paper was edited by Sonja Martens and reviewed by two anonymous referees.

References

Atkins, J. E.: Special reports of freak waves, The Marine Observer, 47, 32–34, 1977.

Auken, S.: Answers in the wind: How Denmark became a world pioneer in wind power, Fletcher Forum of World Affairs, 26, 149–157, 2002.

Bacon, S. and Carter, D. J. T.: Wave climate changes in the North Atlantic and North Sea, Int. J. Climatol., 11, 545–558, https://doi.org/10.1002/joc.3370110507, 1991.

Belfast Telegraph: Dozens die as winds hit continent, 4, 26 January 1990.

Berz, G. A.: Global warming and the insurance industry, in: Cost-Benefit Analysis of Climate Change: The Broader Perspective, edited by: Toch, F. L., Birkhauser Verlag, Basel, Switzerland, 41–56, 1998.

Berz, G. A.: Catastrophes and climate change: concerns and possible countermeasures of the insurance industry, IPCC Workshop, Costa Rica, April 1998, Proceedings. Mitigation and adaptation strategies for the global change, Kluwer Academic Publishers, 4, 283–293, 1999.

Berz, G.: Windstorm and storm surges in Europe: Loss trends and possible counter-actions from the viewpoint of an international reinsurer, Philos. T. Roy. Soc. A, 363, 1431–1440, https://doi.org/10.1098/rsta.2005.1577, 2005.

Beurskens, J.: The History of Wind Energy, Understanding Wind Power Technology: Theory, Deployment and Optimisation, First Edition, edited by: Schaffarczyk, A., John Wiley and Sons, https://media.wiley.com/product_data/excerpt/13/11186475/1118647513-25.pdf (last access: 31 October 2024), 2014.

BODC: UK Tide Gauge Network, https://bodc.ac.uk/data/hosted_data_systems/sea_level/uk_tide_gauge_network/, last access: 29 November 2024.

Bouws, E., Jannink, D., and Komen, G. J.: The increasing wave height in North Atlantic Ocean, B. Am. Meteorol. Soc., 77, 2275–2276, https://doi.org/10.1175/1520-0477(1996)077<2275:TIWHIT>2.0.CO;2, 1996.

British Geological Survey: BGS earthquake database search, https://www.earthquakes.bgs.ac.uk, last access: 21 June 2024.

Buller, P. J. S.: The gales of January and February 1990: damage to buildings and structures, Building Research Establishment Report, Building Research Establishment, Garston, Watford, WD2 7JR, 24 pp., 1993.

Christou, M. and Ewans, K.: Examining a comprehensive dataset containing thousands of freak wave events. Part 1 – Description of the data and quality control procedure, in: Proceedings of the ASME 2011 30th International Conference on Ocean, Offshore and Arctic Engineering, OMAE2011, 19–24 June 2011, Rotterdam, The Netherlands, OMAE2011-50168, 2011.

Corkan, R. H.: The levels in the North Sea associated with the storm disturbance of 8 Jan 1949, Philos. T. Roy. Soc. Lond. A, 242, 493–525, 1950.

Danish Energy Agency: Security of Electricity Supply in Denmark, Danish Energy Agency, Copenhagen, 36 pp., ISBN 978-87-93180-15-4, https://ens.dk/sites/ens.dk/files/Globalcooperation/security_of_electricity_supply_in_denmark.pdf (last access: 1 November 2024), 1st edn. 2015, translated 2016.

Darbyshire, J.: Microseisms and weather, Weather, 53, 342–351, https://doi.org/10.1002/j.1477-8696.1998.tb06341.x, 1998.

de Jong, M. P. C. and Battjes, J. A.: Low-frequency sea waves generated by atmospheric convection cells, J. Geophys. Res., 109, C01011, https://doi.org/10.1029/2003JC001931, 2004.

Deutschen Wetterdienst: Monatlicher Witterungsbericht, 38, 1–2, January 1990.

Ditlevsen, C., Ramos, M. M., Sørensen, C., Ciocan, U. R., and Pionkowitz, T.: Højvandsstatistikker 2017, Miljø- og Fødevareministeriet, Kystdirektoratet, Lemvig, 86 pp., https://kyst.dk/media/bizn2o4z/hoejvandsstatistikker2017revideret11022019.pdf (last access: 1 November 2024), 2018.

Dolezalek, H.: Oceanographic research towers in Europe, ONR Europe Reports, AD-A264 795, 28 pp., https://apps.dtic.mil/sti/tr/pdf/ADA264795.pdf (last access: 1 November 2024), December 1992.

Dorland, C., Tol, R. S. J., Olsthoorn, A. A., and Palutikof, J. P.: Impacts of windstorms in the Netherlands: Present risk and prospects for climate change, in: Climate, Change and Risk, edited by: Downing, T. E., Olsthoorn, A. A., and Tol, R. S. J., Routledge, London and New York, 245–278, 1999.

Draper, L.: "Freak" Ocean Waves, Oceanus, 10, 13–15, 1964.

DWD: Klimatologische Bewertung der jüngsten Starkwindereignisse (ANATOL und LOTHAR) aus der Sicht der Klimatologie der freien Atmosphäre, Deutscher Wetterdienst, 8 pp., https://www.dwd.de/DE/leistungen/besondereereignesse/stuerme/20000201_bewertung_lothar-anatol.html (last access: 1 November 2024), 1 February 2000.

European Severe Weather Database: 25–26 January 1990, https://eswd.eu, last access: 6 November 2023.

Faulkner, D.: Shipping safety. A matter of concern, Ingenia, Royal Academy of Engineering, London, 13, 13–20, 2002.

Franke, R.: Eine Serie von Orkantiefs über der Nord- und Ostsee im Januar/Februar 1990, Wetterlotse, 518, 30–37, February 1990.

Gao, C.: Analysis of storm surge and tidal resonance in the Bristol Channel, M.S., Oxford University, 117 pp., https://users.ox.ac.uk/~spet1235/Thesisfinal-ChanshuGao.pdf (last access: 1 November 2024), 2017.

Gardiner, B.: Appendix 1: List of all Storms in Database, European Forest Institute, Atlantic European Regional Office – EFI-Atlantic, 19 pp., https://ec.europa.eu/environment/forests/pdf/Final_Report_Appendix_1.pdf (last access: 12 January 2023), 2010a.

Gardiner, B.: Appendix 3: Background information on 11 storms selected for detailed analysis, European Forest Institute, Atlantic European Regional Office - EFIAtlantic, 161 pp., https://ec.europa.eu/environment/forests/pdf/Final_Report_Appendix_3.pdf (last access: 3 January 2021), 2010b.

Gatzen, C., Pucik, T., and Ryva, D.: Two cold-season derechoes in Europe, Atmos. Res., 100, 740–748, https://doi.org/10.1016/j.atmosres.2010.11.015, 2011.

Gemmrich, J., Garrett, C., and Thompson, K.: Extreme waves in Canadian coastal waters, in: 11 th International Workshop on Wave Hindcasting and Forecasting and Coastal Hazard Symposium, JCOMM Technical Report 62, WMO/TD-No. 1533, IOC Workshop Report 232, Halifax, Canada, 18–23 October 2009, 8 pp., http://www.waveworkshop.org/11thWaves/Papers/CoastalExtremeWaves_submit.pdf (last access: 1 November 2024), 2009.

Gönnert, G. and Buß, T.: Sturmfluten zur Bemessung von Hochwasserschutzanlagen, Berichte des Landesbetriebes Strassen, Brücken und Gewässer Nr.2/2009, Freie und Hansestadt Hamburg, Landesbetrieb Strassen, Brücken und Gewässer (LSBG), Hamburg, 109 pp., https://lsbg.hamburg.de/resource/blob/784556/2e48879ef0f4403202c675792a11d0a0/bericht-nr-2-sturmfluten-zur-bemessung-von-hochwasserschutzanlagen-data.pdf (last access: 1 November 2024), 2009.

Gönnert, G., Isert, K., Giese, H., and Plüss, A.: Charakterisierung der Tidekurve, Die Küste, 68, 99–141, https://izw.baw.de/die-kueste/0/k068103.pdf (last access: 1 November 2024), 2004.

Grøning, B. Koch, M., Canter, W., and Møller, T.: Vindproduceret El, Naturlig Energi, 12, 16–32, 1990.

Hamre, R., Kvitrud, A., and Tesdal, K.: In service experience of fixed offshore structured in Norway (OMAE-91-512/AQ-305-90/24.9.1990), in: Proceedings of the 10th International Conference on Offshore Mechanics and Arctic Engineering 1991, 23–28 June 1991, Stavanger, Norway, 331–336, http://kvitrud.no/1991OMAEInserviceexperienceoffixedoffshorestructures.pdf (last access: 27 November 2024), 1991.

Hansen, J.: Storms of my Grandchildren, Bloomsbury, New York, 304 pp., ISBN 978-1-60819-200-7, 2009.

Hasager, C. B., Astrup, P., and Nielsen, P.: QuikSCAT and SSM/I ocean surface winds for wind energy, in: IEEE International Geoscience and Remote Sensing Symposium, 2007, IGARSS 2007, 3507–3512, https://doi.org/10.1109/IGARSS.2007.4423602, 2007a.

Hasager, C. B., Astrup, P., Nielsen, M., Christiansen, M. B., Badger, J., Nielsen, P., Sørensen, P. B., Barthelmie, R. J., Pryor, S. C., and Bergstrøm, H.: SAT-WIND project Final Report, Riso-R-1586(EN), Riso National Laboratory, Technical University of Denmark, Roskilde, Denmark, 131 pp., https://backend.orbit.dtu.dk/ws/files/7703216/ris_r_1586.pdf (last access: 1 November 2024), 2007b.

Haver, S.: A possible freak wave event measured at the Draupner Jacket January 1 1995, in: Rogue Waves 2004, Proceedings of a Workshop organized by Ifremer at Brest, 20–22 October 2004, 299–306, https://archimer.ifremer.fr/doc/00716/82826/87648.pdf (last access: 1 November 2024), 2005.

Heipertz, M. and Nickel, C.: Climate change brings stormy days: Case studies on the impact of extreme weather events on public finances, SSRN Electronic Journal, https://doi.org/10.2139/ssrn.1997256, 2008.

Heming, J. T.: The impact of surface and radiosonde observations from two Atlantic ships on a numerical weather prediction model forecast for the storm of 25 January 1990, Meteorol. Mag., 119, 249–259, 1990.

Herald Express: Trail of death nationwide, 1 p., 26 January 1990.

Herklotz, K.: FINO Sea state measurements at FINO1, in: 52nd IEA Topical Expert Meeting. Wind and Wave Measurements at Offshore Locations, Berlin, Germany, 20–21 February 2007, 131–138, https://iea-wind.org/wp-content/uploads/2023/10/52_Wind_Wave.pdf (last access: 1 November 2024), 2007.

Hewson, T. D. and Neu, U.: Cyclones, windstorms and the IMILAST project, Tellus A, 67, 27128, https://doi.org/10.3402/tellusa.v67.27128, 2015.

Houghton, J. T., Jenkins, G. J., and Ephraums, J. J. (Eds.): Climate Change. The IPCC Scientific Assessment, Cambridge University Press, Cambridge, 410 pp., ISBN 0 521 40360 X, https://www.ipcc.ch/site/assets/uploads/2018/03/ipcc_far_wg_I_full_report.pdf (last access: 1 November 2024) , 1990.

International Energy Agency: IEA R&D WECS Annual Report 1980, https://iea-wind.org/wp-content/uploads/2022/12/IEA-Wind-1980-Annual-Report.pdf (last access: 6 December 2024), 25 pp., January 1981.

Jensen, J. and Müller-Navarra, S. H.: Storm surges on the German coast, Die Küste, 74, 92–124, https://henry.baw.de/server/api/core/bitstreams/7c78dedb-1489-4a69-9722-adaa420eb0de/content (last access: 1 November 2024), 2008.

Jensen, P. H. and Winther-Jensen, M.: 99 % af møllerne velbeholdne igennem stormen 25. januar, Naturlig Energi, 12, 6, 1990.

Johns, R. H., Davies, J. M., and Leftwich, P. W.: Some wind and instability parameters associated with strong and violent tornadoes. 2. Variations in the combinations of wind and instability parameters, in: The Tornado: Its Structure, Dynamics, Prediction, and Hazards, Geophysical Monograph 79, edited by: Church, C., American Geophysical Union, Washington D.C., 583–590, https://prod-east-spc.woc.noaa.gov/publications/johns/torparms.pdf (last access: 1 November 2024), 1993.

Joosten, H. P.: Datawell 1961–2011, Drukkerij Grave, Heemstede, 353 pp., https://datawell.nl/wp-content/uploads/2022/10/datawell_jubileumboek_english.pdf (last access: 1 November 2024), 2013.

Kartverket: Se havnivå, https://www.kartverket.no/til-sjos/se-havniva, last access: 29 November 2024.

Kettle, A. J.: Review Article: Storm Britta in 2006: offshore damage and large waves in the North Sea, Nat. Hazards Earth Syst. Sci. Discuss., 3, 5493–5510, https://doi.org/10.5194/nhessd-3-5493-2015, 2015.

Kettle, A. J.: The North Sea surge of 31 October–1 November 2006 during Storm Britta, Adv. Geosci., 45, 273–279, https://doi.org/10.5194/adgeo-45-273-2018, 2018.

Kettle, A. J.: Storm Tilo over Europe in November 2007: storm surge and impacts on societal and energy infrastructure, Adv. Geosci., 49, 187–196, https://doi.org/10.5194/adgeo-49-187-2019, 2019.

Kettle, A. J.: Storm Xaver over Europe in December 2013: Overview of energy impacts and North Sea events, Adv. Geosci., 54, 137–147, https://doi.org/10.5194/adgeo-54-137-2020, 2020.

Kettle, A. J.: Storm Anatol over Europe in December 1999: impacts on societal and energy infrastructure, Adv. Geosci., 56, 141–153, https://doi.org/10.5194/adgeo-56-141-2021, 2021.

Kettle, A. J.: Storm Kyrill and the storms of mid-January 2007: Societal and Energy Impacts in Europe, Adv. Geosci., 58, 135–147, https://doi.org/10.5194/adgeo-58-135-2023, 2023a.

Kettle, A. J.: Storm Franz: Societal and energy impacts in northwest Europe on 11–12 January 2007, Adv. Geosci., 62, 41–55, https://doi.org/10.5194/adgeo-62-41-2023, 2023b.

Kystdirektoratet: Vandstandsmålinger, https://kyst.dk/hav-og-anlaeg/maalinger-og-data/vandstandsmaalinger, last access: 29 November 2024.

Kvitrud, A.: Crest height calculations, document created 2/9/1997, http://kvitrud.no/crest-calculations.htm (last access: 1 November 2024), 1997.

Landesregierung Schleswig-Holstein: Stormfloot und Hochwadder, dat geiht uns al wat an, Wasserstark.SH, https://www.schleswig-holstein.de/DE/landesregierung/themen/kueste-wasser-meer/wasserstarkSH/_documents/__geschichten/jensen.html (last access: 1 November 2024), last update: 27 August 2023.

Liu, P. C.: A chronology of freaque wave encounters, Geofizika, 24, 57–70, 2007.

Liu, P. C. and MacHutchon, K. R.: Are there different kinds of rogue wave? in: Proceedings of OMAE2006, 25th International Conference on Offshore Mechanics and Arctic Engineering, Hamburg, Germany, 4–9 June 2006, OMAE2006-92619, 865–870, 2006.

Lloyd's Weekly Casualty Returns: Vol. 279, No. 4, Lloyd's of London Press Ltd., Sheepen Place, Colchester, Essex, CO3 3LP, 6 February 1990a.

Lloyd's Weekly Casualty Returns: Vol. 279, No. 5, Lloyd's of London Press Ltd., Sheepen Place, Colchester, Essex, CO3 3LP, 13 February 1990b.

Lockwood, J. F., Guentchev, G. S., Alabaster, A., Brown, S. J., Palin, E. J., Roberts, M. J., and Thornton, H. E.: Using high-resolution global climate models from the PRIMAVERA project to create a European winter windstorm event set, Nat. Hazards Earth Syst. Sci., 22, 3585–3606, https://doi.org/10.5194/nhess-22-3585-2022, 2022.

Mallory, J. K.: Abnormal waves on the south east coast of South Africa, Int. Hydrogr. Rev., 51, 99–129, 1974.

Mariners Weather Log: North Atlantic Weather Log January, February and March 1990, Marine Weather Review, Mariners Weather Log, 50–63, 1990.

McCallum, E.: The Burn's Day storm, 25 January 1990, Weather, 45, 166–173, https://doi.org/10.1002/j.1477-8696.1990.tb05607.x , 1990.

McCallum, E. and Norris, W. J. T.: The storms of January and February 1990, Meteorol. Mag., 119, 201–220, 1990.

McRobie, A., Spencer, T., and Gerritsen, H.: The big flood: North Sea storm surge, Philos. T. Roy. Soc. A, 363, 1263–1270, 2005.

Météo France: Daria le 25 janvier 1990, https://web.archive.org/web/20171107022827/http://tempetes.meteofrance.fr/Daria-le-25-janvier-1990.html (last access: 26 March 2023), 2016.

Meteorological Office: Daily Weather Summary, https://www.metoffice.gov.uk/research/library-and-archive/publications/daily-weather-summary (last access: 1 November 2024), 25 January 1990.

Miller, R. C.: Notes on analysis and severe-storm forecasting procedures of the Air Force Global Weather Central, Technical Report 200 (Rev), Air Weather Service (MAC), United States Air Force, 184 pp., https://apps.dtic.mil/sti/tr/pdf/AD0744042.pdf (last access: 1 November 2024), May 1972.

Milwauki Journal: Fierce storm claims 93 lives in Europe, https://onlylivingboyintitirangi.wordpress.com/2013/11/18/weathering-the-burns-day-storm-25-26-january-1990/ (last access: 1 November 2024), 26 January 1990.

Monserrat, S., Vilibić, I., and Rabinovich, A. B.: Meteotsunamis: atmospherically induced destructive ocean waves in the tsunami frequency band, Nat. Hazards Earth Syst. Sci., 6, 1035–1051, https://doi.org/10.5194/nhess-6-1035-2006, 2006.

Neu, H. J. A.: Interannual variations and longer-term changes in sea state of the North Atlantic from 1970 to 1982, J. Geophys. Res., 89, 6397–6402, https://doi.org/10.1029/JC089iC04p06397, 1984.

Nikolkina, I. and Didenkulova, I.: Catalogue of rogue waves reported in media in 2006–2010, Nat. Hazards, 61, 989–1006, https://doi.org/10.1007/s11069-011-9945-y, 2012.

NRC Handelsblad: Zeker 65 doden in buitenland, p. 1, 26 January 1990a.

NRC Handelsblad: Zwaarste windstoten na 1944, p. 3, 26 January 1990b.

NTSLF: Skew surge history: England – east, https://ntslf.org/storm-surges/skew-surges/england-east, last access: 12 October 2024.

O'Brien, L., Dudley, J. M., and Dias, F.: Extreme wave events in Ireland: 14 680 BP–2012, Nat. Hazards Earth Syst. Sci., 13, 625–648, https://doi.org/10.5194/nhess-13-625-2013, 2013.

Olagnon, M. and Athanassoulis, G. A. (Eds.): Rogue Waves 2000, Proceedings of a Workshop organized by Ifremer at Brest 29–30 November 2000, Ifremer, 390 pp., 2001.

Olagnon, M. and Prevosto, M. (Eds.): Rogue Waves 2004, Proceedings of a Workshop organized by Ifremer at Brest 20–22 October 2004, Ifremer, 308 pp., 2005.

Olagnon, M. and Prevosto, M.: Rogue Waves 2008, Proceedings of a Workshop organized by Ifremer at Brest 13–15 October 2008, Ifremer, 296 pp., 2009.

Parsons, A. and Frampton, A.: Cell 1 Regional Coastal Monitoring Programme Wave Data Analysis Report 2: 2013–2014, CH2MHILL Halcrow, Final Report, 122 pp., March 2014.

Pasqualetti, M., Righter, R., and Gipe, P.: History of Wind Energy, in: Encyclopedia of Energy, vol. 6, Elsevier, 419–433, https://www.researchgate.net/publication/265594973_History_of_Wind_Energy (last access: 1 November 2024), 2004.

Pattiaratchi, C. B. and Wijeratne, E. M. S.: Are meteotsunamis an underrated hazard?, Philos. T. Roy. Soc. A, 373, 2140377, https://doi.org/10.1098/rsta.2014.0377, 2015.

Pinto, J. G., Zacharias, S., Fink, A. H., Leckebusch, G. C., and Ulbrich, U.: Factors contributing to the development of extreme North Atlantic cyclones and their relationship with the NAO, Clim. Dynam., 32, 711–737, https://doi.org/10.1007/s00382-008-0396-4, 2009.

Pleskachevsky, A. L., Lehner, S., and Rosenthal, W.: Storm observations by remote sensing and influences of gustiness on ocean

waves and on generation of rogue waves, Ocean Dynam., 62, 1335–1351, https://doi.org/10.1007/s10236-012-0567-z, 2012.

Pugh, D. T.: Tides, Surges and Mean Sea Level, John Wiley and Sons, ISBN 0 471 91505X, 1987.

Rambøll: Kortlægning af Bølgeenergiforhold i den dansk del af Nordsøen, Energistyrelsen J.No. 51191/97-0014, Rambøll, Dansk Hydraulisk Institut, Danmarks Meteorologiske Institut, 133 pp., 4 June 1999.

Roberts, J. F., Champion, A. J., Dawkins, L. C., Hodges, K. I., Shaffrey, L. C., Stephenson, D. B., Stringer, M. A., Thornton, H. E., and Youngman, B. D.: The XWS open access catalogue of extreme European windstorms from 1979 to 2012, Nat. Hazards Earth Syst. Sci., 14, 2487–2501, https://doi.org/10.5194/nhess-14-2487-2014, 2014.

Rosenthal, W.: Results of the Maxwave project, in: Rogue Waves. Proc. 14th 'Aha Huliko' Hawaii, Winter Workshop, 25–28 January 2005, Univ. Hawaii, Manoa, Honolulu, 7 pp., https://www.soest.hawaii.edu/PubServices/2005pdfs/Rosenthal.pdf (last access: 2 November 2024), 2005.

Rosenthal, W. and Lehner, S.: Extreme sea state conditions at offshore platforms, in: 52nd IEA Topical Expert Meeting. Wind and Wave Measurements at Offshore Locations, Berlin, Germany, 20–21 February 2007, 139–150, https://iea-wind.org/task11/tems/ (last access: 2 November 2024), 2007.

RWS: Verslag van de Stormvloed van 25 en 26 januari 1990 (SR62), Ministerie van Veerkeer en Waterstaat, Rijkswaterstaat, Dienst Getijdewateren Stormvloedwaarschuwingsdienst/SVSD, Postbus 20907, 2500 EX 's-Gravenhage, 's-Gravenhage, 24 pp, https://open.rijkswaterstaat.nl/open-overheid/onderzoeksrapporten/%40257220/stormvloedrapporten-kust-benedenrivieren/ (last access: 2 November 2024), April 1990.

RWS: Stormvloedrapport van 5 t/m 7 december (SR91) Sint-Nicolaasvloed 2013, Watermanagementcentrum Nederland, Rijkswaterstaat, prepared by: Kroos, J., 48 pp., https://open.rijkswaterstaat.nl/open-overheid/onderzoeksrapporten/%40257220/stormvloedrapporten-kust-benedenrivieren/ (last access: 2 November 2024), 19 March 2014.

RWS: Rijkswaterstaat Waterinfo, https://waterinfo.rws.nl/#/, last access: 29 November 2024.

Sanders, F. and Gyakum, J. R.: Synoptic-dynamic climatology of the 'Bomb', Mon. Weather Rev., 108, 1589–1606, https://doi.org/10.1175/1520-0493(1980)108<1589:SDCOT>2.0.CO;2, 1980.

Simon, B.: Les niveaux marins extrêmes le long des côtes de France et leur évolution, Service hydrographique et oceanographique de la Marine (SHOM), 139 pp., June 2008.

Slingo, J.: EPA Climate Change Lecture: Facing up to Climate Change: Where next for Climate Science? public lecture at The Round Room, The Mansion House, Dawson St., Dublin 2, https://www.epa.ie/environment-and-you/climate-change/what-is-epa-doing/climate-lectures/ (last access: 3 November 2024), 20 November 2019.

Spencer, T., Brooks, S. M., Evans, B. R., Tempest, J. A., and Möller, I.: Southern North Sea storm surge event of 5 December 2013: Water levels, waves and coastal impacts, Earth-Sci. Rev., 146, 120–145, https://doi.org/10.1016/j.earscirev.2015.04.002, 2015.

Steers, J. A.: The East coast floods 31 January–1 February 1953, in: Applied Coastal Geomorphology, edited by: Steers, J. A., Macmillan, London, 198–223, 1971.

Stull, R. B.: An Introduction to Boundary Layer Meteorology, Kluwer Academic Publishers, Dordrecht, ISBN 978-90-277-2769-5, ISBN 978-90-277-2768-8 (hardcover), 1988.

Supran, G., Rahmstorf, S., and Oreskes, N.: Assess ExxonMobil's global warming projections, Science, 379, eabk0063, https://doi.org/10.1126/science.abk0063, 2023.

SWEB News (South Western Electricity Board monthly newletter): Storm Special, 2–5, February 1990.

Swiss Re: Natural catastrophes and man-made disasters in 2017: a year of record-breaking losses, Sigma No1/2018, Swiss Re Institute, Zurich, Switzerland, 59 pp., https://www.swissre.com/institute/research/sigma-research/sigma-2018-01.html (3 November 2024), 2018.

University of Wyoming: http://weather.uwyo.edu/upperair/sounding.html, last access: 15 August 2023.

US Army Corps of Engineers: Shore Protection Manual, Volume 1, Coastal Engineering Research Center, Department of the Army, Waterways Experiment Station, Corps of Engineers, P.O. Box 631, Vicksburg, Mississippi 39180, USA, 1984.

Wadey, M. P., Haigh, I. D., Nichols, R. J., Brown, J. M., Horsburgh, K., Carroll, B., Gallop, S. L., Mason, T., and Bradshaw, E.: A comparison of the 31 January–1 February 1953 and 5–6 December 2013 coastal flood events around the UK, Front. Mar. Sci., 2, 27, https://doi.org/10.3389/fmars.2015.00084, 2015.

WASA Group: Changing waves and storms in the Northeast Atlantic, B. Am. Meteorol. Soc., 79, 741–760, https://doi.org/10.1175/1520-0477(1998)079<0741:CWASIT>2.0.CO;2, 1998.

Wentz, F. J., Hilburn, K. A., and Smith, D. K.: Remote Sensing Systems DMSP SSM/I Daily Environmental Suite on 0.25 deg grid, Version 7, Remote Sensing Systems, Santa Rosa, California, http://www.remss.com/missions/ssmi (last access: 3 November 2024), 2012.

Wetteronline: Vor 30 Jahren: Orkantief Daria wütet – Tote und Millardenschäden, contributor Matthias Habel, https://www.presseportal.de/pm/12322/4499208 (last access: 3 November 2024), 22 January 2020.

Wubs, A. J. and Waaldijk, A.: Krantelknipsels storm 25 january 1990, Deel 1: Knipsels 1 t/m 200, (Projectnaam: Storm 25-1-90; Projectnummer: 62.8.3903), Instituut TNO voor Bouwmaterialen en Bouwconstructies (IBBC), June 1990.

Zemunik, P., Šepić, J., Pellikka, H., Ćatipović, L., and Vilibić, I.: Minute Sea-Level Analysis (MISELA): a high-frequency sea-level analysis global dataset, Earth Syst. Sci. Data, 13, 4121–4132, https://doi.org/10.5194/essd-13-4121-2021, 2021.